Friction Boosted by Equilibrium Misalignment of Incommensurate Two-Dimensional Colloid Monolayers

Davide Mandelli,[1] Andrea Vanossi,[2,1] Nicola Manini,[3,1,2] and Erio Tosatti[1,2,4]
[1]International School for Advanced Studies (SISSA), Via Bonomea 265, 34136 Trieste, Italy
[2]CNR-IOM Democritos National Simulation Center, Via Bonomea 265, 34136 Trieste, Italy
[3]Dipartimento di Fisica, Università degli Studi di Milano, Via Celoria 16, 20133 Milano, Italy
[4]International Centre for Theoretical Physics (ICTP), Strada Costiera 11, 34151 Trieste, Italy
(Received 8 October 2014; revised manuscript received 13 December 2014; published 10 March 2015)

Colloidal two-dimensional monolayers sliding in an optical lattice are of recent importance as a frictional system. In the general case when the monolayer and optical lattices are incommensurate, we predict two important novelties, one in the static equilibrium structure, the other in the frictional behavior under sliding. Structurally, realistic simulations show that the colloid layer should possess in full equilibrium a small misalignment rotation angle relative to the optical lattice, an effect so far unnoticed but visible in some published experimental moiré patterns. Under sliding, this misalignment has the effect of boosting the colloid monolayer friction by a considerable factor over the hypothetical aligned case discussed so far. A frictional increase of similar origin must generally affect other incommensurate adsorbed monolayers and contacts, to be sought out case by case.

DOI: 10.1103/PhysRevLett.114.108302 PACS numbers: 68.35.Af, 68.35.Gy, 82.70.Dd, 83.10.Rs

The mutual sliding of crystalline lattices offers, despite its apparently academic nature, one of the basic platforms to understand the nanoscale and mesoscale frictional and adhesion phenomena [1]. In one of the freshest developments, Bohlein and collaborators [2] showed that the sliding of a two-dimensional crystalline monolayer of colloidal particles in an optical lattice provides unexpected information on elementary tribological processes in crystalline sliding systems with ideally controlled commensurabilities. Given the scarcity of reliable and controllable frictional systems, it is hard to overestimate the importance of such model systems with full external control over all parameters including periodicity, coupling strengths, and applied forces. For this reason two-dimensional monolayers in periodic lattices require a close theoretical study. In this Letter we describe two main surprises, one structural and one frictional, that emerge from realistic molecular dynamics simulations. We show first of all that incommensurate colloid islands naturally develop in full equilibrium a small misalignment angle relative to the substrate. Second, sliding simulations demonstrate that the misaligned angular orientation increases significantly the dynamic friction with respect to the (hypothetical and unstable) aligned case. While both are important for colloidal monolayers, their potential impact extends in principle beyond the specific case, to a wider variety of systems where mutually incommensurate two-dimensional lattices are brought in static and then in sliding contact.

In colloid monolayers, the two-dimensional density may vary from "underdense" ($\rho < 1$, where $\rho = a_l/a_c$ with a_l the spacing of the optical lattice and a_c that of the colloid lattice, both triangular) to perfectly commensurate ($\rho = 1$, one particle per potential well), to "overdense" ($\rho > 1$), each with its specific sliding behavior. Both experiments [2] and theory [3,4] indicated that commensurate ($\rho = 1$) friction is large, dropping to much lower values for $\rho \neq 1$, where the optical and colloid lattices are incommensurate. This drop reflects the great mobility of the preexisting misfit dislocations, also called kinks or "solitons." In these studies the two lattices, colloid and optical, were silently assumed to be geometrically aligned, prior to and during sliding. That assumption however is dangerous. A long-known theoretical result suggests [5], for example, that a harmonic monolayer subject to an incommensurate periodic potential of weak amplitude U_0 may partly convert the misfit compressional stress to shear stress by an equilibrium geometric misalignment of the monolayer (see Fig. 1) through a small rotation angle

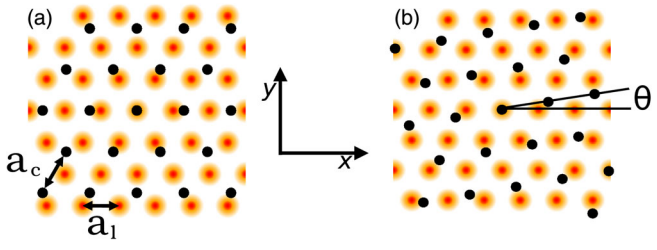

FIG. 1 (color online). (a) Schematic of a two-dimensional colloidal lattice (black dots) aligned with an incommensurate triangular periodic potential mimicking the optical lattice (blurred spots represent potential minima). (b) A misaligned configuration rotated by an angle θ.

$$\theta_{\mathrm{NM}} = \arccos\left(\frac{1+\rho^2(1+2\delta)}{\rho[2+\delta(1+\rho^2)]}\right), \quad (1)$$

whose energy-lowering effect originates from a better interdigitation of the two lattices. Independent of U_0, the rotation angle is nonzero in this approximation provided the transverse two-dimensional sound velocity c_T is sufficiently smaller than the longitudinal c_L, precisely if $\delta = (c_L/c_T)^2 - 1 > \rho^{-1}$. While this kind of rotated epitaxy has been addressed experimentally [6,7] and theoretically [8] for adsorbed rare-gas monolayers, its possible presence in colloidal monolayers was so far unsuspected. More importantly in the context of sliding friction, the tribological impact of an equilibrium geometrical misalignment is unexplored in any incommensurate system. The externally forced rotation turning a commensurate layer into an incommensurate one is well known to reduce friction, as exemplified by the sliding of graphene flakes on graphite [9,10]. Different as these two cases are, a possible expectation might be that the equilibrium geometry, alignment of commensurate layers, or misalignment of incommensurate layers, should always exhibit a higher friction relative to forcedly rotated ones, since the optimal $T = 0$ geometry must in every case correspond to a closer interdigitation of the two lattices.

First, let us consider structural alignment. Using the same methods as in Ref. [[3]], we model the colloidal system in an optical lattice as a two-dimensional monolayer of N_p pointlike classical particles, mutually repelling through a screened Coulomb potential $U_{\mathrm{pp}}(r_{ij})$ while immersed in a static two-dimensional triangular lattice potential $W(\mathbf{r}_i) = U_0 w(\mathbf{r}_i)$, where $w(\mathbf{r}_i)$ is a dimensionless periodic function of spacing a_l (as specified in the Supplemental Material [11]), and U_0 is the amplitude ("corrugation") parameter. The Hamiltonian is thus

$$H = \sum_{i=1}^{N_p}\left[U_0 w(\mathbf{r}_i) + \frac{1}{2}\sum_{j\neq i} U_{\mathrm{pp}}(r_{ij})\right]. \quad (2)$$

The particles are confined to the (x, y) plane, and subjected to either planar periodic boundary conditions (PBCs) in a given area A, or alternatively to an additional Gaussian confining potential $G(r) = -A_G \exp(-r^2/\sigma_G^2)$, in which case they form an island with open boundary conditions (OBCs). Temperature is generally set to zero, because the results are clearer and require less statistics in this limit. Finite temperature results are otherwise not essentially different, as shown along with details of optimization protocols in the Supplemental Material [11]. Within the confinement region the two-dimensional particles crystallize in a triangular lattice of mean spacing a_c, with modulations induced by the periodic potential (in the OBC case there is also a confinement-induced variation between a dense center and a sparser periphery). Here and in the rest, we shall focus for specificity on the underdense incommensurate case $\rho = 3/(1+\sqrt{5}) \simeq 0.927$; the physics with different values of $\rho \neq 1$ including $\rho > 1$ is qualitatively similar, as briefly discussed in the Supplemental Material [11].

We determined, by means of careful energy minimization, the optimal $T = 0$ two-dimensional geometry of all N_p particles for increasing corrugation strength; shown here are the results for $U_0 = 0.1$–0.6, where the effects are particularly clear. The final, optimal geometry of the two-dimensional colloid lattice initially aligned at $\theta = 0°$ with the optical lattice axes is found to be misaligned, with a small rotation angle $\theta_{\mathrm{opt}} \simeq 2.3°$ in PBC calculations. This rotation realizes a better interdigitation with the optical lattice, and occurs spontaneously during the simulation at the cost of creating the dislocations required by the PBC constraints (see the Supplemental Material [11]). More detailed energy minimizations were done in OBC, which do not have the same problem. Since the 30 000 particle islands are too large to spontaneously rotate, we carried out simulations starting from a prearranged sequence of misalignment angles. The total energy minimum versus θ confirms, as shown by Fig. 2, the structural misalignment angle at equilibrium, with a magnitude in the range $3° < \theta_{\mathrm{opt}} < 5°$ (depending on the optical lattice strength U_0) generally somewhat larger than in PBC, where angular constraints hinder the misalignment.

These structural results compare instructively with those expected from the harmonic model [5]. In our case a two-dimensional phonon calculation for the monolayer yields a sound velocity ratio $c_L/c_T = 1.806$, larger than the theoretical threshold value $(1+\rho^{-1})^{1/2} \simeq 1.442$. The corresponding theoretical misalignment $\theta_{\mathrm{NM}} \simeq 2.6°$ is in qualitative agreement with the more realistic simulation result. Figures 2(b) and 2(c) show how the two pieces that compose the total energy, namely, the periodic lattice energy part $W = \langle W(\mathbf{r}_i)\rangle$ controlled by the corrugation amplitude U_0 and the interparticle interaction $U_{\mathrm{pp}} = \langle U_{\mathrm{pp}}(r_{ij})\rangle$, behave. Misalignment raises the interparticle energy, but that cost is overcompensated, by a factor of 2, by a corrugation energy gain. The incommensurate colloid static equilibrium structure is misaligned because that permits a better interdigitation with the optical lattice.

Even if our predicted misalignments are small, their experimental existence is easily revealed, because the rotation angle θ between two lattices is highly amplified by the moiré pattern, which rotates relative to the periodic potential lattice by an angle ψ satisfying the geometric relation $\cos\theta = \rho^{-1}\sin^2\psi + \cos\psi[1-\rho^{-2}\sin^2\psi]^{1/2}$ [12]. As the moiré superlattice rotates by ψ, its spacing L also decreases [13] from its aligned value of about $L = a_c\rho/(1-\rho)$ to its rotated value of $L' = a_c/\sqrt{1+\rho^{-2}-2\rho^{-1}\cos\theta}$. As an example, Fig. 3 reports the structures of the artificially unrotated and of the

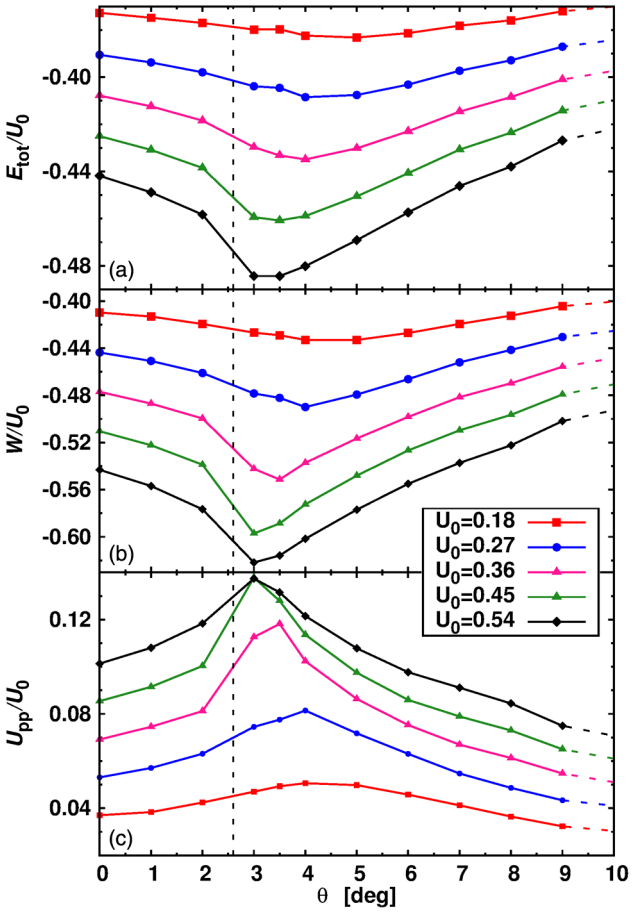

FIG. 2 (color online). Relative static energy of structure-optimized colloid islands (OBC) as a function of the trial rotation angle θ. (a) Total energy per particle $E_{\rm tot}$. (b) Periodic-potential (corrugation) contribution W to $E_{\rm tot}$. (c) Interparticle interaction contribution $U_{\rm pp}$ to $E_{\rm tot}$. Curves correspond to increasing corrugation amplitude $U_0 = 0.18$–0.54. Energies are measured relative to that of the colloidal monolayer at rest and at $U_0 = 0$. Dashed line: ideal NM angle [Eq. (1)] $\theta_{\rm NM} \approx 2.6°$.

optimally rotated ($\theta_{\rm opt} = 7°$) configurations calculated for $\rho \simeq 0.83$ and $U_0 = 6.3$ (parameters believed to be appropriate to experiments in Ref. [14]) in comparison with one another and with the corresponding experimental structural moiré pattern. Both the orientation and spacing of Fig. 3(c) agree with the $\theta_{\rm opt} = 7°$ but not with the $\theta_{\rm opt} = 0°$ pattern, proving that the misalignment was actually present in that experiment.

The particle static displacements associated with the optical lattice potential are also enlightening. Figure 4 shows the moiré pattern of a small portion of the monolayer island ($\rho = 0.927$, $U_0 = 0.27$) for $\theta = 0°$ and for $\theta_{\rm opt} = 4°$, corresponding to a moiré angle $\psi \approx 15°$. Particle displacements, designated by arrows, change from longitudinal compression dilations to mixed shear-longitudinal, vortex-like displacements upon optimal misalignment. A large two-dimensional bulk modulus and a weak shear rigidity of

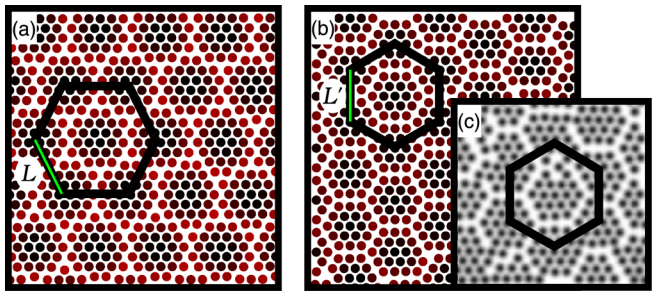

FIG. 3 (color online). Equilibrium configurations obtained for $\rho \simeq 0.83$ and $U_0 = 6.3$. (a) Unrotated $\theta = 0°$ and (b) optimally rotated $\theta_{\rm opt} = 7°$. Dark (light) colloids enjoy best (worse) W. Only the central part of the island, optimized in OBC, is shown. (c) Experimental geometry for the same ρ, adapted from Ref. [14], where both the moiré angles and spacing compare directly with (b) rather than (a).

the crystalline monolayer are crucial factors increasing the extent of the shear distortions, therefore enhancing the lattice misalignment.

We come to our second point, i.e., the forced sliding of the particle monolayer over the periodic corrugation and the associated frictional losses. The shear distortions and the corresponding increased interdigitation at the optimal misalignment angle $\theta_{\rm opt}$ are expected to affect the sliding of the particle lattice over the periodic potential. Sliding is realized by a flow of the soliton superstructure, accompanied by dissipation as part of the work goes into soliton-related time-dependent distortions of the two-dimensional lattice. That work will change once the nature (longitudinal to shear), orientation (0° to ψ), and periodicity (L to L') change with θ (0° to $\theta_{\rm opt}$). We determine the magnitude of the expected friction change by simulating the overdamped sliding dynamics of the OBC island over a range of θ values, so as to assess the frictional effect of misalignment near its optimal value. We applied an external driving force F_d acting on each particle, slowly varying to and fro as a function of time, mimicking the experimental drag force ηv_d induced by a fluid of viscosity η and slowly back and forth time-dependent speed v_d [2] (details in the Supplemental Material [11]). Despite a nonzero torque, generally present for all preset angles that differ from $\theta_{\rm opt}$ (and from zero) the misalignment angle did not have the time to change appreciably in the course of the simulation. Under sliding, the frictional power dissipated per particle was calculated as [3]

$$p_{\rm fric} = \mathbf{F_d} \cdot \langle \mathbf{v}_{\rm cm} \rangle - \eta |\langle \mathbf{v}_{\rm cm} \rangle|^2 = (\eta/N_p) \Sigma_i \langle |\mathbf{v}_i - \mathbf{v}_{\rm cm}|^2 \rangle, \quad (3)$$

where $\mathbf{v}_{\rm cm}$ is the center-of-mass velocity, $\mathbf{v}_i$ is the velocity of particle i, and brackets denote steady-state averages. Because of the confining envelope potential, the lattice spacing a_c, close to constant in the central part, increases toward the periphery, where colloids also tend to be pinned by the corrugation. To address properties of mobile colloids

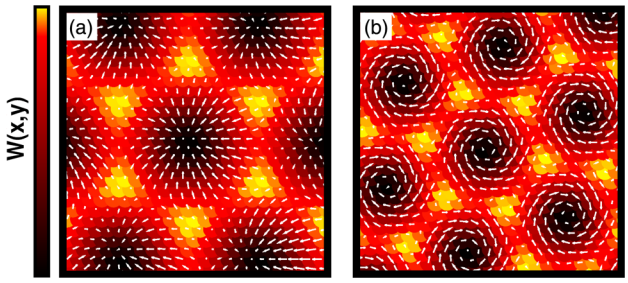

FIG. 4 (color online). Moiré patterns of the particle monolayer's central region as obtained in OBC for $\rho = 0.927$, $U_0 = 0.27$ (a) for $\theta = 0°$ (moiré angle $\psi = 0°$) and (b) for the optimal $\theta = 4°$ (moiré angle $\psi \approx 15°$). Each dot indicates a particle in the unrelaxed configuration, colored according to the local corrugation potential $W(\mathbf{r})$: dark for potential minima, bright for maxima. White arrows show the displacements of each particle from the ideal triangular lattice to the fully relaxed configuration, magnified 15 times. The compressions-dilations at $\theta = 0°$ are turned into largely shear, vortexlike displacements at $\theta_{\text{opt}} = 4°$.

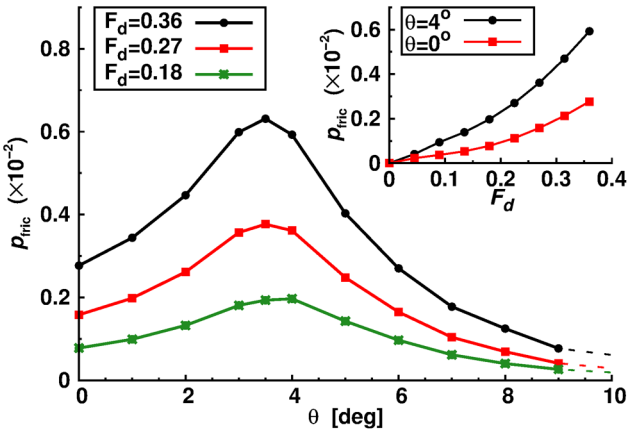

FIG. 5 (color online). Dissipated friction power p_{fric} as a function of the trial misalignment angle θ ($U_0 = 0.27$). Three curves are reported corresponding to increasing values of the driving force $F_d = 0.18, 0.27, 0.36$. The inset shows p_{fric} as a function of F_d for two values of θ.

at a well-defined density, trajectories were analyzed, as is also done in experiments, considering only particles belonging to the central portion of the island, in our case a square of size $80 \times 80 a_c^2$. The duration of the sliding simulations was fixed by requiring a total center-of-mass displacement not smaller than $\Delta x_{\text{cm}} \approx 2$–$3 a_c$.

Figure 5, our main dynamical result, shows that friction is increased by a very substantial factor by misalignment relative to alignment, reaching a maximum of about 2 at the optimal angle θ_{opt}, subsequently dropping for larger angles where the energy gain and static distortion magnitude also drop. The physical reason for the frictional peak at θ_{opt} can be further appreciated by looking at the particles' steady-state velocity distribution P_v and at the corresponding static interparticle spacing distribution (at zero velocity) P_r, both shown in Fig. 6 for increasing θ. The important points here are that small interparticle distances are energetically costly, and that a large spread of velocities relative to the center of mass denotes larger frictional dissipation, according to the rhs of Eq. (3). At perfect alignment, short distances (colored column) are very frequent, which is energetically costly. At the same time the spread of velocities is moderate and so is friction. In the optimally misaligned case θ_{opt} instead, the shortest distance becomes less frequent, thus reducing energy as we already know. At the same time however P_v develops longer tails at lower and higher particle velocities, both of which increase friction. At $\theta > \theta_{\text{opt}}$ finally the velocity spread drops and so does friction, the monolayer sliding being less and less affected by corrugation.

In conclusion, colloid monolayers in an incommensurate optical lattice develop, in full equilibrium and with realistic parameters, a small-angle structural misalignment, quite evident in moiré patterns such as those of Fig. 3. Upon forced sliding, this misalignment can considerably increase the sliding friction, directly extractable from the colloid drift velocity in experiment, using Eq. (3), over the hypothetical aligned geometry.

The present results and understanding naturally extrapolate to the sliding of misaligned incommensurate lattices in contact such as, for example, physisorbed rare-gas or molecular submonolayer islands [6–8]. An interesting side aspect is in this case that misalignment transforms the orientation angle of a physisorbed island, generally assumed to be fixed, into a continuous and possibly dynamical variable. The inertial sliding friction of such

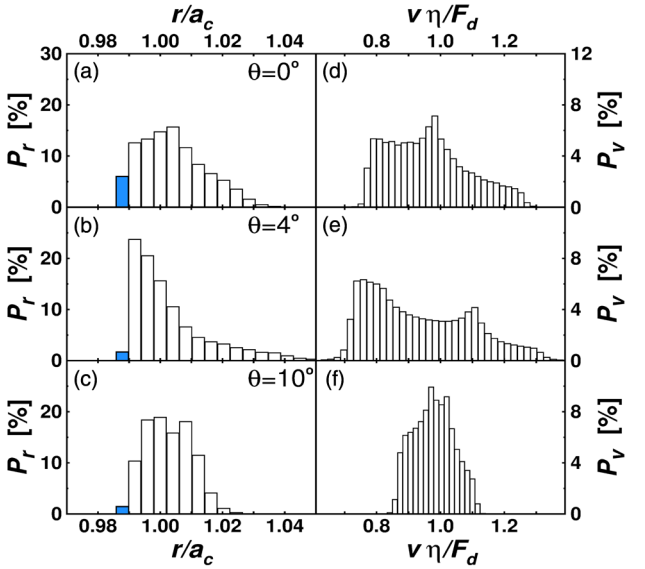

FIG. 6 (color online). (a)–(c) The distribution P_r of nearest-neighbor distances in the static relaxed configurations ($F_d = 0$, $U_0 = 0.27$) at rotation angles $\theta = 0°$, $\theta = \theta_{\text{opt}} = 4°$, and $\theta = 10°$. (d)–(f) Corresponding velocity distribution P_v of particles sliding under an external force $F_d = 0.36$.

islands determines the inverse slip time in quartz crystal microbalance experiments [15], whose data must, at least in some cases, embed the frictional enhancement caused by misalignment when present. Even though the time needed to diffusively rotate an ~100-nm-size island may be exceedingly large, the orientation angle distribution of islands will usually, under either stationary or sliding conditions, be continuous rather than delta-function-like. Our general ignorance of the two-dimensional lattice orientations of incommensurate rare gas islands (as opposed to full monolayers, whose epitaxy generally differs) poses at present an obstacle to the investigation of these effects, which must nonetheless be considered as generically present and effective. The possible local misalignment of incommensurate three-dimensional crystals in contact and its potential role in sliding friction is an even less explored, but interesting issue, which remains open for future consideration.

This work was mainly supported under ERC Advanced Grant No. 320796-MODPHYSFRICT, and partly by the Swiss National Science Foundation through SINERGIA Contract No. CRSII2_136287, by PRIN/COFIN Contract No. 2010LLKJBX 004, and by COST Action MP1303.

[1] A. Vanossi, N. Manini, M. Urbakh, S. Zapperi, and E. Tosatti, Rev. Mod. Phys. **85**, 529 (2013).
[2] T. Bohlein, J. Mikhael, and C. Bechinger, Nat. Mater. **11**, 126 (2012).
[3] A. Vanossi, N. Manini, and E. Tosatti, Proc. Natl. Acad. Sci. U.S.A. **109**, 16429 (2012).
[4] J. Hasnain, S. Jungblut, A. Trster, and C. Dellago, Nanoscale **6**, 10161 (2014).
[5] A. D. Novaco and J. P. Mc Tague, Phys. Rev. Lett. **38**, 1286 (1977).
[6] C. G. Shaw, S. C. Fain, and M. D. Chinn, Phys. Rev. Lett. **41**, 955 (1978).
[7] T. Aruga, H. Tochihara, and Y. Murata, Phys. Rev. Lett. **52**, 1794 (1984).
[8] M. S. Tomassone, J. B. Sokoloff, A. Widom, and J. Krim, Phys. Rev. Lett. **79**, 4798 (1997).
[9] M. Dienwiebel, G. S. Verhoeven, N. Pradeep, J. W. M. Frenken, J. A. Heimberg, and H. W. Zandbergen, Phys. Rev. Lett. **92**, 126101 (2004).
[10] A. E. Filippov, M. Dienwiebel, J. W. M. Frenken, J. Klafter, and M. Urbakh, Phys. Rev. Lett. **100**, 046102 (2008).
[11] See Supplemental Material at http://link.aps.org/supplemental/10.1103/PhysRevLett.114.108302 for a description of calculational details, including optimization protocols.
[12] F. Grey and J. Bohr, Europhys. Lett. **18**, 717 (1992).
[13] P. San-Jose, A. Gutièrrez-Rubio, M. Sturla, and F. Guinea, Phys. Rev. B **90**, 075428 (2014).
[14] S. Bleil, H. H. von Grünberg, J. Dobnikar, R. Castañeda-Priego, and C. Bechinger, Europhys. Lett. **73**, 450 (2006).
[15] J. Krim, Adv. Phys. **61**, 155 (2012).